JTTEES 6:327-334

Oxides in Plasma-Sprayed Chromium Steel

K. Volenik, J. Leitner, F. Hanousek, J. Dubsky, and B. Kolman

Products of oxidation reactions accompanying plasma spraying of chromium steel by a water-stabilized plasma gun were separated from the metallic matrix by a chemical method. This enabled gravimetric determination of the oxide content in plasma-sprayed chromium steel and characterization of the composition and structure of oxides by diffraction and spectroscopic techniques. Both the random and inherent errors of the gravimetric method were estimated. The phase composition of oxides was compared with the results of thermodynamic calculations. It was shown that in spite of the highly nonequilibrium character of plasma spraying, the thermodynamic approach can yield useful predictions for the overall phase composition and for the stoichiometry of the prevailing spinel oxide phase.

Keywords chromium steel, equilibrium calculations, gravimetry, oxidation, phase analysis, plasma spraying

1. Introduction

Plasma spraying of metals is usually accompanied by oxidation reactions, which result in formation of oxides in the coatings (Ref 1-5). An analysis of metallic (iron) particle oxidation in flight and after impact on the substrate was given (Ref 6).

The presence of oxides in metallic coatings is usually undesirable because they deteriorate the coating properties. To assess these effects and to eventually avoid or decrease the oxidation, it is necessary to determine the quantity of oxides, their composition, and structure.

The present paper is mainly concerned with the following problems: thermodynamic considerations (section 2), gravimetric determination of oxide amounts (section 3.2), and the composition and structure of oxides (section 3.3).

A comparison of the results obtained in sections 2 and 3.3 in this article indicates the probability of using the thermodynamic approach to predict the oxide phases obtained during a highly nonequilibrium process such as plasma spraying.

2. Thermodynamic Considerations

2.1 *System Description*

Though the plasma-spraying conditions differ from thermodynamic equilibrium, calculation of the equilibrium composition of the systems being reviewed yields useful information. Knowledge of which phases are thermodynamically stable under the given conditions, that is, which phases can result from chemical reactions accompanying plasma spraying, is particularly useful. In addition, the dependence of individual phase equilibrium amount on the initial conditions allows assessment of the effect of spraying parameters on the presence of these phases in real systems. References 7-9 give published results of equilibrium calculations for some plasma processes.

Though some minor elements, such as manganese and molybdenum, are present in chromium steel, preliminary analyses of oxides resulting from plasma spraying (section 3.3.1) showed that the only elements important in oxidation were iron, chromium, and silicon. To simplify the problem, further considerations are limited to the ternary Fe-Cr-Si metallic system.

Table 1 lists the substances involved in the calculations and the references giving the initial thermodynamic data. Ideal behavior of the gaseous phase is suggested.

The model of a substitutional solution was applied to describe the ternary alloy Fe-Cr-Si in bcc, fcc, and liquid phases.

Table 1 Substances involved in equilibrium calculations. List of relevant references

Phase	Components	Input thermodynamic data: Pure substances	Input thermodynamic data: Mixing properties
Gas	Fe,FeO,Cr,CrO, CrO_2,CrO_3,Si,SiO, O,O_2,H,H_2,H_2O	Ref 10	Ideal solution
Liquid metal	Fe,Cr,Si	Ref 11	Fe-Cr, Ref 12 Fe-Si, Ref 13 Cr-Si, Ref 14
Liquid oxide	FeO,$CrO_{1.5}$,SiO_2	Ref 10	Ideal solution
bcc	Fe,Cr,Si	Ref 11	Fe-Cr, Ref 12 Fe-Si, Ref 15 Cr-Si, Ref 14
fcc	Fe,Cr,Si	Ref 11	Fe-Cr, Ref 12 Fe-Si, Ref 15 Cr-Si ideal solution
Spinel	$FeCr_2O_4$,Fe_3O_4	Ref 10	Ideal solution
Corundum	Cr_2O_3,Fe_2O_3	Ref 10	Ref 16
Single component phases	$Fe_{0.947}O$	Ref 10	...
	Si	Ref 11	...
	SiO_2	Ref 10	...
	$FeSiO_3$	Ref 10	...
	Fe_2SiO_4	Ref 10	...
	FeSi	Ref 10	...
	$FeSi_2$	Ref 10	...
	CrSi	Ref 14	...
	$CrSi_2$	Ref 14	...
	Cr_3Si	Ref 14	...
	Cr_5Si_3	Ref 14	...

bcc, body-centered cubic; fcc, face-centered cubic

K. Volenik, J. Dubsky, and **B. Kolman,** Institute of Plasma Physics ASCR, Za Slovankou 3, P.O. Box 17, 182 00, Praha 8, Czech Republic; **J. Leitner,** Department of Solid State Engineering, Institute of Chemical Technology, Technická 5, 166 28 Praha 6, Czech Republic; **F. Hanousek,** Institute of Inorganic Chemistry ASCR, 250 68 Rez u Prahy, Czech Republic.

To express the dependence of the excess Gibbs energy on the solution composition, the method suggested by Muggianu et al. (Ref 17) for the calculation of binary contributions determined by the Redlich-Kister equation (Ref 18) was used. The solubility of oxygen in the alloy was not tested.

The description of the oxide melt and the solid (Fe,Cr)oxide phases was based on the sublattice model (Ref 19). The corundum-type $Fe_{2-x}Cr_xO_3$ and the spinel-type $Fe_{3-y}Cr_yO_4$ are further referred to as "corundum" and "spinel," respectively. For the melt and spinel, ideal mixing conditions were assumed. The description of the deviations from ideal mixing for corundum was based on the regular solution model.

Ferrous oxide $Fe_{1-z}O$ was considered stoichiometric in the liquid phase ($z = 0$); whereas, the average deviation from stoichiometry $z = 0.053$ was adopted for the solid phase (wüstite).

2.2 *Equilibrium Calculations*

A method based on minimizing the total Gibbs energy of the system for a set of points satisfying the material balance conditions was used to calculate the equilibrium composition of the systems Fe-Cr-Si-O-N-H. The method and the corresponding computer program CHEMEQ have been previously described (Ref 20).

Equilibrium composition was calculated for various initial compositions of the systems under consideration in the temperature range of 1000 to 3000 K at the total pressure $p/p^0 = 1$ (p^0 = 101.325 kPa). The suggested initial amount of the solid alloy ($n^0[s]$) was 10 mol. The composition (Fe-13wt%Cr-0.8wt%Si) was chosen in approximate agreement with the chromium and silicon concentrations in the feedstock powder. The initial amount of the gaseous phase ($n^0[g]$) was varied in the range of 1

Table 2 Equilibrium amounts (mol) of condensed phases in the system Fe-Cr-Si-O

Temperature, K	Phase	$n^0(g)/n^0(s)$ 0.1	0.2	0.3	0.4	0.5	0.6
1000	bcc	8.719	7.000	5.500	4.000	2.500	0.646
	Spinel	...	0.844	1.344	1.844	2.344	2.395
	Corundum	0.563	...	...	...	...	...
	$Fe_{0.947}O$	...	...	...	...	...	1.795
	SiO_2	0.156	...	...	...	...	...
	Fe_2SiO_4	...	0.156	0.156	0.156	0.156	0.156
1500	bcc	8.719	...	...	...	...	...
	fcc	...	7.078	5.300	3.406	1.512	...
	Spinel	...	0.922	1.069	1.069	1.069	1.554
	Corundum	0.563	...	...	...	...	...
	$Fe_{0.947}O$	...	...	1.412	3.412	5.412	5.472
	SiO_2	0.156	0.156	0.156	0.156	0.156	0.156
2000	Spinel	...	0.347	...	...	...	1.650
	Corundum	0.458	...	...	...	...	...
	Liq-Me	8.684	6.826	4.831	2.838	0.841	...
	Liq-Ox	0.401	2.133	5.169	7.162	9.159	5.051
2500	Liq-Me	8.501	6.724	4.796	2.824	0.838	...
	Liq-Ox	1.499	3.276	5.204	7.176	9.162	9.999
3000	Liq-Me	8 272	6.608	4.726	2.791	0.830	...
	Liq-Ox	1.591	3.392	5.274	7.209	9.170	9.976

Table 3 Equilibrium amounts (mol) of condensed phases in the system Fe-Cr-Si-O-N ($n^0(O_2):n^0(N_2)$ = 21:79)

Temperature, K	Phase	$n^0(g)/n^0(s)$ 0.1	0.2	0.3	0.4	0.5	0.6
1000	bcc	9.772	9.492	9.212	8.932	8.652	8.322
	Spinel	...	...	...	...	...	0.151
	Corundum	0.036	0.176	0.316	0.456	0.596	0.535
	SiO_2	0.156	0.156	0.156	0.156	0.156	0.156
1500	bcc	9.771	9.491	9.211	8.932	...	...
	fcc	...	...	...	...	8.652	8.314
	Spinel	...	...	...	...	...	0.175
	Corundum	0 039	0.178	0.317	0.457	0.596	0.502
	SiO_2	0.152	0.153	0.154	0.155	0.156	0.156
2000	Spinel	...	...	...	...	...	0.145
	Corundum	0 048	0.167	0.282	0.390	0.473	0.337
	Liq-Me	9.742	9.465	9.187	8.905	8.608	8.243
	Liq-Ox	1.604	0.200	0.248	0.313	0.442	0.646
2500	Liq-Me	9.665	9.332	8.970	8.608	8.236	7.853
	Liq-Ox	2.642	0.568	0.882	1.221	1.567	1.925
3000	Liq-Me	7.430	5.719	4.148	2.635	1.149	...
	Liq-Ox	...	0.249	0.538	0.850	1.176	1.519

to 6 mol. The ratio $n^0(g)/n^0(s) < 1$ was chosen to simulate the situation where the oxidation reaction occurs on the metallic particle surfaces only. Three different gaseous phase compositions were considered: oxygen, air (21% O_2, 79% N_2), and a mixture of oxygen with hydrogen (1:2). The latter gas mixture is noted for spraying conditions, which use a water-stabilized plasma gun, because plasma is generated by dissociation and ionization of water in this particular case. The main focus of the calculations was to determine the equilibrium phase composition of each particular system and the equilibrium partial pressure of O_2 in the gaseous phase.

Tables 2-4 and Fig. 1 summarize the results of the calculations. The tables present the equilibrium moles of the phases being studied and allow assessment of the significance of the content of a phase at equilibrium conditions. The tables also show cases where a phase is absent. Figure 1 gives the equilibrium partial pressure of oxygen as a function of temperature in the system Fe-Cr-Si-O-H. Usually, the number of coexisting phases is <5; that is, the corresponding number of degrees of freedom is >0. It follows that the equilibrium oxygen partial pressure depends on the initial gaseous phase amount.

3. Experimental

3.1 *Samples*

Chromium steel was plasma deposited on cylindrical rods (30 mm diam) of plain steel (Czechoslovak standard CSN 11373) by a water-stabilized plasma gun PAL 160 (Institute of Plasma Physics ASCR, Praha, Czech Republic). The following concentrations (wt%) of the main alloying elements in the chromium steel feedstock powder (CSN 17021) were obtained by chemical analysis: Cr 13.2, Mn 1.5, Mo 1.3, Ni 0.2, and Si 0.8. Particle dimensions were in the range of 0.10 to 0.14 mm. The basic plasma-spraying parameters were spraying distance 300 mm, feeding distance 65 mm, feed rate 0.53 kg/min, shrouding gas nitrogen at 30 L/min, and substrate cooling by argon. The coating density was 6.81 g/cm^3.

Figure 2 shows the distribution of oxides in the chromium steel coating. White areas correspond to the metallic phase, gray spots correspond to oxides, and black spots correspond to pores

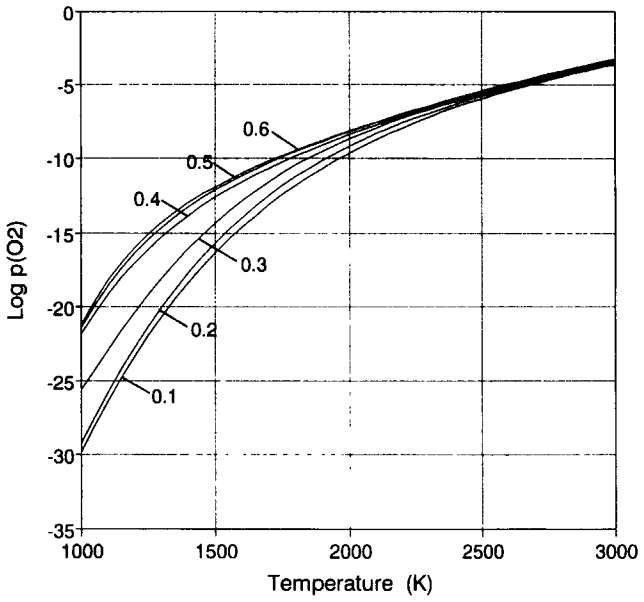

Fig. 1 Equilibrium partial pressure of oxygen in the system Fe-Cr-Si-O-H as a function of temperature. The value of $n^0(g)/n^0(s)$ is given for each curve. The composition of the gaseous phase corresponds to $n^0(O_2):n^0(H_2) = 1{\cdot}2$. The initial amount of the metallic phase is 10 mol [$n^0(Fe) = 8.472$ mol, $n^0(Cr) = 1.372$ mol, $n^0(Si) = 0.156$ mol].

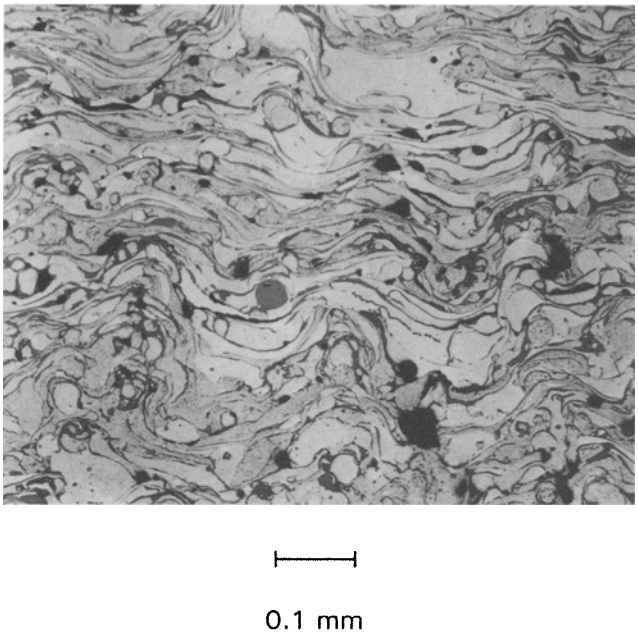

Fig. 2 Optical micrograph of a cross section of plasma-sprayed chromium steel coating

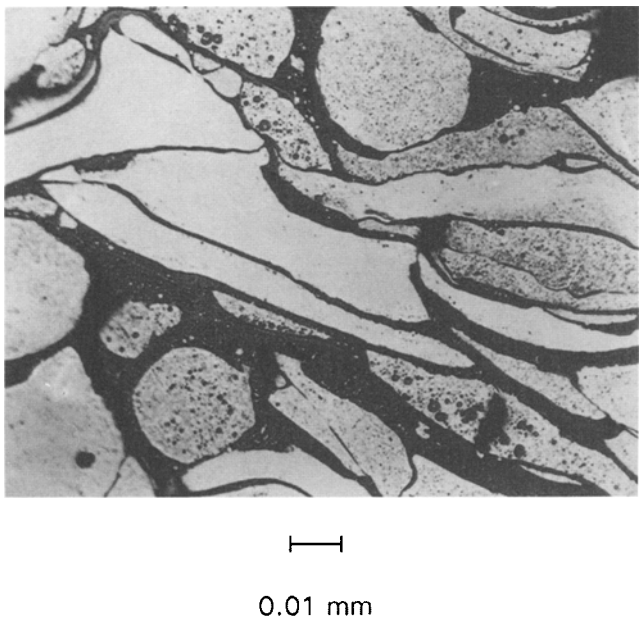

Fig. 3 Optical micrograph of a cross section of plasma-sprayed chromium steel coating. Higher magnification than in Fig. 2

Table 4 Equilibrium amounts (mol) of condensed phases in the system Fe-Cr-Si-O-H ($n^0(O_2):n^0(H_2)$ = 1:2)

Temperature, K	Phase	$n^0(g)/n^0(s)$ 0.1	0.2	0.3	0.4	0.5	0.6
1000	bcc	9.385	8 719	7.847	7.400	6.962	6.525
	Spinel	...	. .	0.625	0 742	0.856	1.002
	Corundum	0.229	0.563	0 061	...	...	...
	SiO_2	0.156	0.156	0.156	0.046	...	...
	Fe_2SiO_4	...	...	...	0.110	0.156	0.156
1500	bcc	9.387	8.729	...	...	...	...
	fcc	...	...	7.941	7 707	7.518	7.281
	Spinel	...	...	0.548	0.713	0.775	0.854
	Corundum	0.230	0.558	0.130	..	. .	...
	SiO_2	0.154	0.156	0.156	0.156	0.156	0.156
2000	Spinel	...	...	0.187	0.490	0.372	0.206
	Corundum	0.196	0.424	0.295	...	...	...
	Liq-Me	9.395	8.805	8.200	7.563	6.936	6.227
	Liq-Ox	0.212	0.347	0.647	0.966	1.946	3.151
2500	Liq-Me	9.345	8.681	8.011	7.335	6.652	5.963
	Liq-Ox	0.582	1.206	1.843	2.487	3.139	3.796
3000	Liq-Me	6.553	4.183	1 954	...	...	...
	Liq-Ox	0.257	0.796	1.374	1.970	2.528	3.034

and voids. A higher magnification (Fig. 3) enables observation of a large number of very fine oxide particles dispersed in the metallic phase.

It is not practical to study in detail the composition and structure of oxides dispersed in the metallic matrix (Fig. 2, 3). To extract the oxides from the metallic matrix, a chemical method consisting of dissolving the metallic phase in an iodine-methyl alcohol solution was used. This method had been frequently used for separating surface oxide films from iron-base metals where it dissolved a thin underlying metallic layer. For the present study, however, it was necessary to dissolve the bulk metallic matrix. This was achieved using machining to remove the coating, except for a thin layer near the coating-substrate interface, and by treating the machined turnings in a solution of iodine in methyl alcohol (100 g/L). The water content in methyl alcohol p.a. was 0.06%. Desiccation of methyl alcohol by prolonged boiling with elemental magnesium did not produce any significant effect on the reaction products. The kinetics of chromium steel dissolution were very slow, although a number of solution temperatures up to the boiling point of methyl alcohol were tested. A rotating jar with a reflux condenser at 60 °C was found to be the most efficient treatment method. The dissolution of ~4 g of crushed turnings in ~700 mL of solution took approximately 9 h.

It was difficult to extract oxide particles from the suspension as obtained by metallic matrix dissolution. Multiple dilution with alcohol followed by sedimentation was ineffective. Centrifugation was applicable; nevertheless, large losses could not be avoided. The best results with minimum losses were obtained by pressure filtering through a suitable membrane that was insoluble in methyl alcohol and contained pores 2 μm in diameter (obtained by DDS-RO Division, A/S de Danske Sukkerfabrikker, Nakskov, Denmark). This was followed by drying at an elevated temperature.

3.2 *Gravimetric Determination of Oxide Amount*

To determine the oxide content in thermally sprayed coatings, a microscopic method based on the measurement of the oxide cross-section area sum is usually used. In the present paper, an attempt was made to determine the oxide content by weighing the oxidation products separated from the plasma deposited steel using the chemical method previously described.

For chromium steel, which was plasma sprayed using the previously described method, five independent dissolution runs gave the following oxide content in the coating (95% confidence limits):

$$m_{ox} = (13.6 \pm 0.6)\ wt\%$$

To assess the systematic errors, the following additional experiments were conducted:

- Possible losses due to extremely small particles passing through the membrane filter pores were checked by repeated filtering through a membrane filter with a pore diameter of 0.5 μm. No traces of oxide powder on the filter were observed.
- Losses occurring during suspension handling and the resulting oxide powder, due to adhesion of very fine oxide particles to all solid surfaces, were determined by a repeated soaking and filtering procedure employing the oxide powder previously separated from the metallic matrix. The oxide losses were as great as 25 mg, a value that is almost independent of the batch. This means that for a 4 g batch of turnings, the actual oxide amount will be up to 0.6% higher than the previously given m_{ox} value.
- Mössbauer spectroscopy enabled detection of the undissolved residual metallic αFe phase. The upper limit of this amount can be estimated at ≈5% (section 3.3.4). X-ray diffraction revealed the presence of the most intense diffraction line of αFe. Its intensity corresponded to the ferritic phase concentration of 2.8 wt% (section 3.3.2). The larger of these two values indicates that the corresponding inherent error was up to 0.7 wt% of the batch.
- The possible presence of by-products (iron or chromium iodides, or hydroxides) accompanying the dissolution of the metallic phase was assessed by weighing the solid products of the dissolution of unsprayed feedstock powder. The

mean amount of this product was 0.5% of the batch, which can be taken as the maximum possible value because it includes oxides present on the surface of feedstock powder particles before spraying.

It can be concluded that the prevailing inherent error originates from the residual metallic phase present in separated oxides. Additional milling and a repeated dissolution procedure applied to oxides previously separated did not significantly change the content of the residual metallic phase. Figure 3 shows that this phase is identical with bright particles embedded in gray oxide matrix. The oxide envelope causes the metallic particles to be inaccessible to the liquid and prevents dissolution.

The value obtained by the microscopic method based on the measurement of the sum of the oxide cross-section areas was $m_{ox} = 9.0\%$. This is considerably lower than the value obtained gravimetrically. The difference is probably due to the microscopic method, which did not account for extremely fine oxide particles embedded in the metallic matrix.

3.3 *Composition and Structure of Oxides*

The elemental composition of oxides obtained by the previously described separation procedure was determined by x-ray fluorescence (XRF) analysis. The phases present in the oxides were studied by x-ray diffraction, infrared spectroscopy, and Mössbauer spectroscopy.

3.3.1 X-Ray Fluorescence Analysis

The elemental analysis of oxides was performed by an energy dispersive XRF analyzer LINK XR 200 (LINK Analytical Ltd., High Wycombe, U.K.) with a rhodium anode tube at 25 kV, with a current of 50 μA, and a preset analysis time of 100 s. The energy dispersive spectra were calibrated using CuO.

The qualitative analysis determined that the predominant elements (other than oxygen) present in the oxides were chromium, iron, and silicon. The conventional method of calculating the concentrations of elements from x-ray intensities resulted in an improbably high concentration of silicon as the lightest element. It was necessary to employ another method for the determination of element concentrations from x-ray intensity data, in particular, a procedure using standard specimens.

The oxides separated from plasma-sprayed coatings contained some minor elements, mainly manganese and molybdenum. However, concentrations did not exceed those in the metallic matrix. These elements were considered to have little importance for oxidation compared to chromium and silicon, which were more abundant in the oxides than in the metallic matrix and with iron as a base element in the matrix alloy. Further considerations were limited to the ternary Cr-Fe-Si system.

A number of techniques applicable for standard specimen preparation were tested. To minimize the results scatter, pellets (14 mm diam) prepared by pressing a mixture of oxide powder (60 mg) with polymethylmethacrylate powder (240 mg) at 130 °C were used. Both standard specimens and those containing oxides separated from plasma-sprayed coatings were prepared using the same method.

Standard specimens were made of powders of pure Fe_2O_3, Cr_2O_3, and SiO_2. The particle size analysis of these powders indicated mean particle dimensions (50 wt% average) of 0.91, 1.73, and 1.63 μm, respectively. In the oxides separated from plasma-sprayed coatings, the predominant phase was $Fe_{3-y}Cr_yO_4$, where $y \approx 1.9$ (sections 3.2.3, 4). However, this oxide was not available for the standard specimen preparation. It was replaced by a mixture of Fe_2O_3 and Cr_2O_3. Considering XRF analysis, there is a difference between this mixture and the previously mentioned phase because of a slightly different oxygen content. The resulting difference in x-ray absorption was not tested in the present analyses.

The first step consisted of the determination of the Cr/Fe ratio in separated oxides. For this purpose, a set of standard specimens containing only Cr_2O_3 and Fe_2O_3 in the range (wt%) of 55:45 (Cr/Fe = 1.20) to 75:25 (2.94) was prepared. From a calibration curve based on the x-ray intensity ratios, a Cr/Fe ratio equal to 1.81 was determined in the separated oxides.

The second step considered the ternary Cr-Fe-Si system. The assumption of a constant ratio of chromium and iron x-ray intensities allowed this system to be treated as a pseudo-binary system (Ref 21). For the previously mentioned ratio of chromium and iron, a set of ternary standard specimens in the range of 2 to 8 wt% SiO_2 was prepared. From a calibration curve (ratio of x-ray intensities $I_{Si}/(I_{Cr} + I_{Fe} + I_{Si})$ plotted against silicon concentration), the value of 2.8 wt% was determined for silicon concentration in the Cr-Fe-Si system for the separated oxides.

If oxygen is not taken into account, and the sum of all minor element concentrations (predominantly manganese and molybdenum) is set at 4 wt%, then the concentrations of major elements in separated oxides are 60.1 wt% Cr, 33.2 wt% Fe, and 2.7 wt% Si.

3.3.2 X-Ray Diffraction Analysis

The x-ray diffraction qualitative phase analysis was performed by a diffractometer Siemens D 500 (Siemens AG, Instrumentation and Control Division, Karlsruhe, Germany). Filtered chromium radiation was used to suppress the secondary radiation due to chromium present in the oxides.

The qualitative analysis indicated that the dominate phase was a spinel-type oxide Me_3O_4. A comparison with data obtained from other structure sensitive methods indicated that this oxide was $Fe_{3-y}Cr_yO_4$. There were also minor phases present, in particular a low concentration of wüstite and the residual ferritic phase.

The composition of the dominate spinel-type oxide can be characterized in more detail by an exact measurement of the lattice constant. However, this measurement was not conducted because the lattice constant in $Fe_{3-y}Cr_yO_4$ depends on y in a complex manner (Ref 22, 23). To assess the value of y, Mössbauer spectroscopy (section 3.3.4) and, in particular, infrared spectroscopy (section 3.3.3) are more suitable.

To determine quantitatively the content of the residual ferritic phase, the reference intensity ratio of αFe and $FeCr_2O_4$ diffraction lines was calculated using the computer program LAZY PULVERIX (Ref 24). The differences between $FeCr_2O_4$ and the previously mentioned oxide, in which the actual value of y was not equal to 2 (sections 3.3.3, 3.3.4, and 4), and between αFe and chromium steel were not tested. The diffraction lines (110)αFe and (311)$FeCr_2O_4$ were used in the calculation. The result

shows that the content of the ferritic phase in the separated oxides was 2.8 wt%.

3.3.3 Infrared Spectroscopy

The infrared spectra were measured by a grating spectrometer PYE-UNICAM 9512 (Cambridge, UK) in the range of 4000 to 200 cm^{-1}. The oxide powder separated from the plasma-sprayed coating was measured in TlBr pellets. TlBr is more suitable for this purpose than conventional KBr, for which the refractive index is too low.

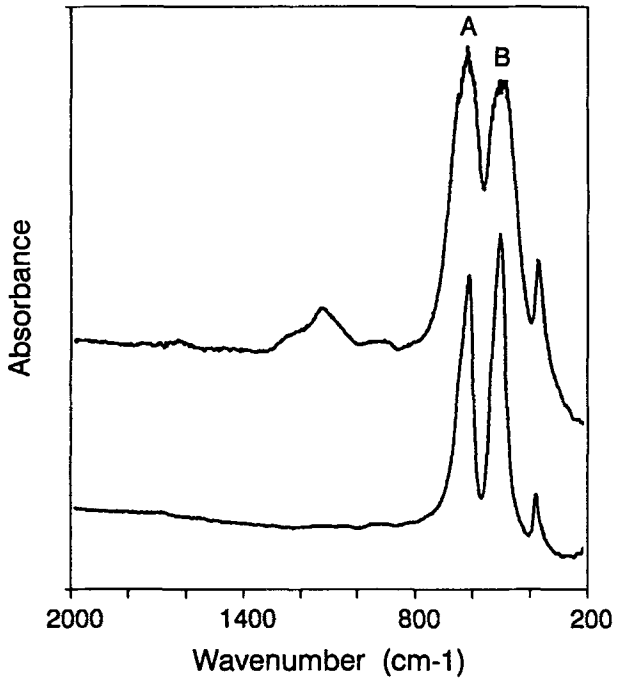

Fig. 4 Infrared spectrum of oxides separated from plasma-sprayed chromium steel (upper curve) as compared with the infrared spectrum of $Fe_{1.04}Cr_{1.96}O_4$ (lower curve, Ref 25)

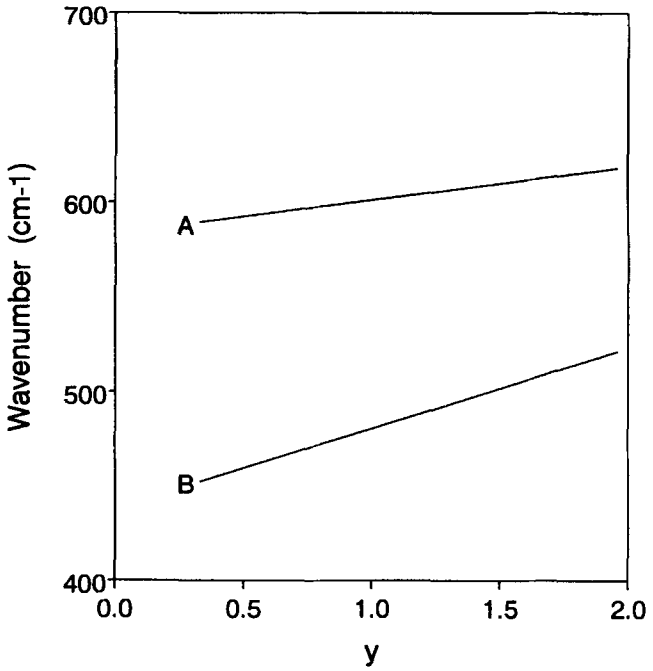

Fig. 5 Wave numbers corresponding to infrared absorption bands A and B (Fig. 4) plotted against y in $Fe_{3-y}Cr_yO_4$ (Ref 25)

In Fig. 4, the significant region of the infrared spectrum of oxides separated from the plasma-sprayed coating (2000 to 200 cm^{-1}) is compared with the same spectral region of synthetic spinel oxide $Fe_{1.04}Cr_{1.96}O_4$ (Ref 25). Both spectra are similar, and their shape is characteristic of the normal spinel structure. The band at 614 cm^{-1} and the broader band at ≈496 cm^{-1} correspond to the stretching modes of Fe-O for iron situated in tetrahedral and octahedral sites. The bands strongly shift to higher wave numbers with respect to the bands corresponding to the same modes in the inverse spinel Fe_3O_4. This is a result of chromium atoms substituted for iron in octahedral sites. The wave numbers corresponding to both bands depend linearly on y in $Fe_{3-y}Cr_yO_4$ (Fig. 5, Ref 25).

The sharp band at 366 cm^{-1} can be attributed to the stretching vibration Cr-O for chromium in octahedral sites because it only appears if $y > 1$.

Another band near 1100 cm^{-1}, with a shoulder at 1198 cm^{-1}, is visible in the infrared spectrum of separated oxides. This band is characteristic of the stretching vibration Si-O in SiO_2, probably in the tridymite modification. This can also explain the broadening of the spinel band at ≈496 cm^{-1} due to the Si-O band superposition at 480 cm^{-1}.

It can be concluded that two oxide phases were detected by infrared spectroscopy. The predominant phase is spinel oxide $Fe_{3-y}Cr_yO_4$, where y equals 1.90 to 1.95. The minor phase is SiO_2 which is present as tridymite.

3.3.4 Mössbauer Spectroscopy

The Mössbauer spectra were measured in a constant velocity mode by a KFKI spectrometer (Institute of Physics, Budapest, Hungary) connected on line with a Canberra FMCA analyzer. The activity of ^{57}Co source in a palladium matrix was 2.5 mCi. The velocity was calibrated by αFe (99.999%).

The Mössbauer spectrum (Fig. 6) of a typical specimen of separated oxides consists of two intense doublets corresponding to a paramagnetic phase and several weak sextets. One of the lat-

Table 5 Mössbauer parameters of superimposed spectral components (Fig. 6)

Phase	Spectral component	Isomer shift, mm/s	Quadrupole splitting, mm/s	Magnetic splitting, Tesla
Spinel	Doublet	0.896 ± 0.003	1.953 ± 0.015	...
Spinel	Doublet	0.880 ± 0.003	0.793 ± 0.018	...
αFe	Sextet	-0.054 ± 0.008	...	32.938 ± 0.059

Table 6 Equilibrium values of y in $Fe_{3-y}Cr_yO_4$

Temperature, K	y in $Fe_{3-y}Cr_yO_4$		
	$n^0(g)/n^0(s) = 0.4$	$n^0(g)/n^0(s) = 0.5$	$n^0(g)/n^0(s) = 0.6$
1000	1.85	1.60	1.37
1500	1.93	1.77	1.61
2000	1.98	1.97	1.94

ter sextets can be attributed to metallic αFe, and the other two weaker sextets are most probably due to Fe_3O_4. The Voight (Lorentz-Gauss) shape of spectral lines was assumed. Comparing the central region of the spectrum with Ref 26, it can be concluded that the doublets correspond to the spinel oxide $Fe_{3-y}Cr_yO_4$, where the value of y is between 1.56 and 1.96. For y = 1.96 or 2.0, the doublets would be so narrow that their superposition would produce an apparent singlet. Table 5 lists the Mössbauer parameters of the previously mentioned spectral components. Two poorly defined sextets of Fe_3O_4 are not given. The line shape in Fig. 6 is a superposition of the spectral components given in Table 5; that is, both sextets attributed to Fe_3O_4 are omitted.

The ratio of the Lamb-Mössbauer factors of αFe and $Fe_{3-y}Cr_yO_4$ is not known; nevertheless, the upper limit of αFe concentration in the mixture of all phases present can be estimated at 5%.

4. Discussion

The separation of oxides from the plasma-sprayed chromium steel by the described chemical method eliminated the interference of a major part of the metallic matrix and allowed for examination of the oxide composition.

The presence of a spinel-type $(Fe,Cr)_3O_4$ as the dominate oxide phase in the separated oxides was indicated unambiguously. No traces of corundum-type $(Fe,Cr)_2O_3$ were detected. As for the spinel-type oxide $(Fe,Cr)_3O_4$, it was possible to assess the value of y in the formula $Fe_{3-y}Cr_yO_4$. The results of infrared and Mössbauer measurements gave $y \approx 1.9$.

A somewhat different value was determined from the XRF analysis, even with the assumption that the iron and chromium in separated oxides were in the spinel-oxide phase, namely y = 1.98. It is obvious that the composition of the major oxide phase was near $FeCr_2O_4$.

In a previous paper (Ref 27), equilibria in a simplified Fe-Cr-O-H system were calculated. In the present paper, systems containing metallic elements as well as silicon in a proportion corresponding to steel composition are considered. Among them, the Fe-Cr-Si-O-H system is noted because it corresponds closely to practical plasma-spraying conditions. The experimental results are in good agreement with the thermodynamic data obtained for this system with the assumption that the ratio of the initial amounts of gaseous and solid phases is $n^0(g)/n^0(s) \geq 0.4$.

The calculations indicate that for these conditions, the prevailing oxide phase below 2000 K is solid spinel oxide $(Fe,Cr)_3O_4$. From the thermodynamic data, the ratio of Cr/Fe concentrations in this spinel oxide (or the value of y in the spinel oxide formula) can be derived. Table 6 gives the values of y for higher initial amounts of the gaseous phase and for the temperature range of 1000 to 2000 K. It shows good agreement with the experiment for $n^0(g)/n^0(s) = 0.4$ in the entire temperature range or for 2000 K in the entire $n^0(g)/n^0(s)$ range.

The presence of traces of wüstite is due to oxidation at a certain stage occurring on a chromium-depleted alloy surface. If wüstite is formed, Fe_3O_4 can result from its decomposition below approximately 830 K during cooling.

The previously described gravimetric method appears to be suitable for determining the oxide content in plasma-sprayed steel. The random errors of the results appear to be acceptable. Some inherent errors mentioned in section 3.2 of this article have opposite signs. It can be assumed that for the plasma-sprayed steel described in this paper, the superimposed inherent errors of the oxide content determination would not exceed ≈1 wt% of the batch.

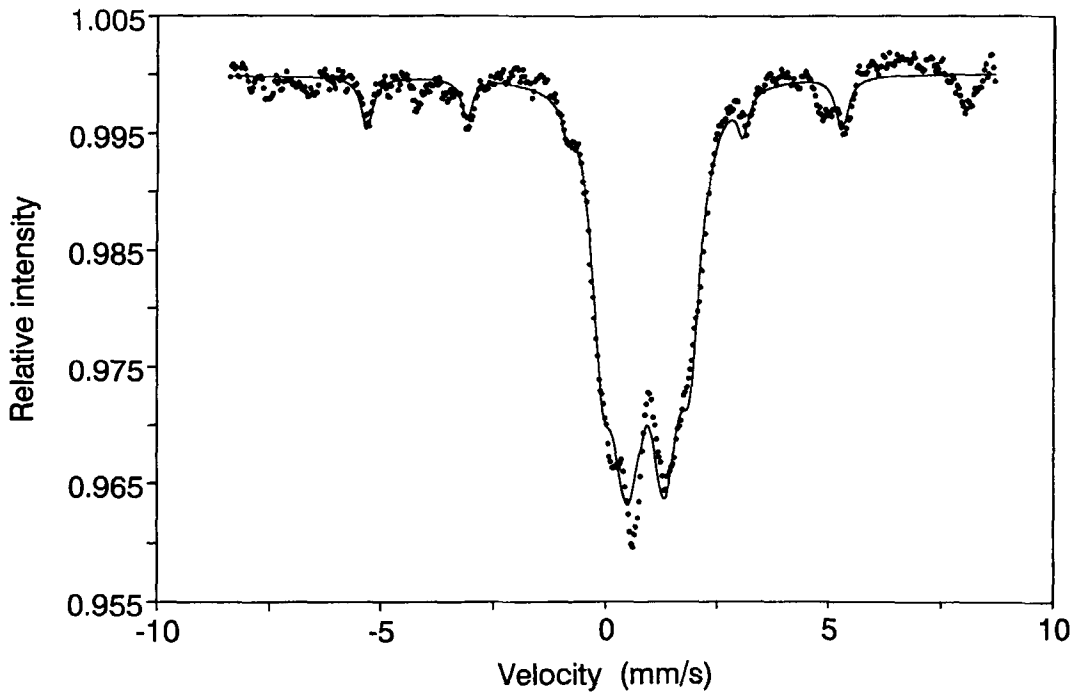

Fig. 6 Mössbauer transmission spectrum of oxides separated from plasma-sprayed chromium steel

5. Conclusions

Plasma-sprayed chromium steel containing high level of oxides was chosen to reveal the advantages and disadvantages of the chemical method of oxide separation. The goal of further investigation will be to decrease the oxide content as much as possible and, thereby, to optimize the plasma-spraying parameters. To better understand the oxidation reactions during plasma spraying, the phenomena occurring in flight and after the molten droplet impingement on the substrate surface must be considered separately.

The oxide presence can be determined by the previously described gravimetric method. The combined diffraction and spectroscopic methods are suitable for studying the composition and structure of chemically separated oxides.

Acknowledgments

The calculations enabling quantitative determination of the content of the residual ferritic phase (section 3.3.2) were conducted by J. Fiala (ŠKODA Research, Plzen). The present work was supported by the grants GACR 106/93/0638 and AV K 1010601/96.

References

1. V. Palka, M. Brezovsky, J. Ivan, and J. Sith, Identification of the Oxides in Plasma Sprayed APS Coating of the NiCrAlY Type, *Thermal Spray: International Advances in Coatings Technology,* C.C. Berndt, Ed., ASM International, 1992, p 537-542
2. P. Siitonen, T. Kinos, and P.O. Kettunen, Corrosion Properties of Stainless Steel Coatings Made by Different Methods of Thermal Spraying, *1994 Thermal Spray Industrial Applications,* C.C. Berndt and S. Sampath, Ed., ASM International, 1994, p 105-110
3. C.M. Hackett and G.S. Settles, Turbulent Mixing of the HVOF Thermal Spray and Coating Oxidation, *1994 Thermal Spray Industrial Applications,* C.C. Berndt and S. Sampath, Ed., ASM International, 1994, p 307-312
4. P. Cheang, Quantitative Analysis of Thermally Sprayed Coatings Using Backscattered Electron Imaging, *1994 Thermal Spray Industrial Applications,* C.C. Berndt and S. Sampath, Ed., ASM International, 1994, p 715-720
5. Z. Zhang, W. Geng, A. Liu, and J. Wen, The Influence of Spray Distance on the Structure and Properties of Arc Sprayed 13% Steel Coatings, *Thermal Spraying Current Status and Future Trends,* A. Ohmori, Ed., High Temperature Society of Japan, Osaka, Japan, 1995, p 1197-1202
6. A. Vardelle, P. Fauchais, and N.J. Themelis, Oxidation of Metal Droplets in Plasma Sprays, *Advances in Thermal Spray Science and Technology,* C.C. Berndt and S. Sampath, Ed., ASM International, 1995, p 175-180
7. J.M. Mexmain, D. Morvan, E. Bourdin, J. Amouroux, and P. Fauchais, Thermodynamic Study of the Ways of Preparing Silicon, and Its Application to the Preparation of Photovoltaic Silicon by the Plasma Technique, *Plasma Chem. Plasma Process.,* Vol 3 (No. 4), 1983, p 393-420
8. N.S. Srinivasan, S. Santén, and L.-I. Staffansson, Plasmochrome Process for Ferrochrome Production—Thermochemical Modeling and Application to Process Data, *Steel. Res.,* Vol 59 (No. 4), 1987, p 151-156
9. P.R. Taylor, S.A. Pirzada, and M Manrique, Thermodynamic Predictions for Material Processing in a Plasma Reactor Using Solid Oxide Feed Materials, *Metall. Mater. Trans. B,* Vol 25 (No. 5), 1994, p 713-720
10. I. Barin, *Thermochemical Data of Pure Substances,* 2nd ed., VCH, Weinheim, 1993
11. A.T. Dinsdale, SGTE Data for Pure Elements, *Calphad,* Vol 15 (No. 4), 1991, p 317-425
12. J.O Andersson and B. Sundman, Thermodynamic Properties of the Fe-Cr System, *Calphad,* Vol 11 (No 1), 1987, p 83-92
13. R. Hultgren, P.D. Desai, P.D. Hawkins, M. Gleiser, and K.K. Kelley, *Selected Values of Thermodynamic Properties of Binary Alloys,* American Society for Metals, 1973, p 871-879
14. C.A Coughanowr, I. Ansara, and H.L. Lukas, Assessment of the Cr-Si System, *Calphad,* Vol 18 (No. 2), 1994, p 125-140
15. T.B Massalski, H. Okamoto, and P.R. Subramanian, *Binary Alloy Phase Diagrams,* 2nd ed., ASM International, 1990, p 1772
16. A.D. Pelton, H. Schmalzried, and J. Sticher, Computer-Assisted Analysis and Calculation of Phase Diagrams of the Fe-Cr-O, Fe-Ni-O, and Cr-Ni-O Systems, *J. Phys. Chem. Solids,* Vol 40 (No. 12), 1979, p 1103-1122
17. Y.-M. Muggianu, M. Gambino, and J.-P. Bros, Enthalpies of Formation of Liquid Alloys Bismuth-Gallium-Tin at 723 K. Choice of an Analytical Representation of Integral and Partial Excess Function of Mixing, *J. Chim. Phys.,* Vol 72 (No. 1), 1975, p 83-88
18. O. Redlich and A.T. Kister, Algebraic Representation of Thermodynamic Properties and the Classification of Solutions, *Ind. Eng. Chem.,* Vol 40 (No. 2), 1948, p 345-348
19. M. Hillert and L.-I. Staffansson, The Regular Solution Model for Stoichiometric Phases and Ionic Melts, *Acta Chem. Scand.,* Vol 24 (No. 10), 1970, p 3618-3626
20. P. Vonka and J Leitner, Calculation of Chemical Equilibria in Heterogeneous Multicomponent Systems, *Calphad,* Vol 19 (No. 1), 1995, p 25-36
21. R. Tertian and F. Claisse, Principles of Quantitative X-Ray Fluorescence Analysis, Heyden, 1982, p 214-216
22. M.H. Francombe, Lattice Changes in Spinel-Type Iron Chromites, *J. Phys. Chem. Solids,* Vol 3 (No. 1), 1957, p 37-43
23. M. Robbins, G.K. Wertheim, R.C. Sherwood, and D.N.E. Buchanan, Magnetic Properties and Site Distributions in the System $FeCr_2O_4$-Fe_3O_4, *J. Phys.,* Colloque 32, C 1, 1971, p 266-267
24. K. Yvon, W. Jeitschko, and E. Parthé, LAZY PULVERIX, A Computer Program for Calculating X-Ray and Neutron Diffraction Powder Patterns, *J. Appl. Crystallogr.,* Vol 10, 1977, p 73-74
25. K. Voleník, F. Hanousek, and B. Strauch, The Infrared Spectra of Solid Solutions of Some Iron and Chromium Oxides, *Czech. J. Phys.,* Vol 31B (No. 1), 1981, p 86-95
26. K. Voleník and M. Seberíni, Mössbauer Spectroscopy of Some Phases in the Fe-Cr-O System and Oxide Layers on Fe-Cr Alloys, *Rev. Cienc. Quim.,* Vol 14 (No. 2), 1983, p 319-333
27. J. Leitner and K. Voleník, Thermodynamics of Oxidation Reactions Accompanying Plasma Spraying of Chromium Steels, *High Temp. Mater. Sci.,* Vol 35 (No. 2), 1996, p 139-150